

Unique phase diagram with narrow superconducting dome in $\text{EuFe}_2(\text{As}_{1-x}\text{P}_x)_2$ due to Eu^{2+} local magnetic moments

Y. Tokiwa, S.-H. Hübner, O. Beck, H.S. Jeevan, and P. Gegenwart

I. Physikalisches Institut, Georg-August-Universität Göttingen, 37077 Göttingen, Germany

(Dated: October 30, 2018)

The interplay between superconductivity and Eu^{2+} magnetic moments in $\text{EuFe}_2(\text{As}_{1-x}\text{P}_x)_2$ is studied by electrical resistivity measurements under hydrostatic pressure on $x = 0.13$ and $x = 0.18$ single crystals. We can map hydrostatic pressure to chemical pressure x and show, that superconductivity is confined to a very narrow range $0.18 \leq x \leq 0.23$ in the phase diagram, beyond which ferromagnetic (FM) Eu ordering suppresses superconductivity. The change from antiferro- to FM Eu ordering at the latter concentration coincides with a Lifshitz transition and the complete depression of iron magnetic order.

After the discovery of high- T_c superconductivity in iron-based materials,¹ tremendous amount of research has been performed on its properties.²⁻⁴ Following the discovery in $\text{LaFeAs}(\text{O},\text{F})$ with $T_c = 26$ K,¹ superconductivity was found in many materials with related crystal structures, that commonly possess iron-pnictide or iron-chalcogenide layers. Like in the cuprates and heavy fermion metals superconductivity of the iron-based compounds has an intimate relation to magnetism. The maximal T_c is found in the vicinity of the extrapolated point where spin-density-wave (SDW) order of the Fe $3d$ magnetic moment is suppressed by pressure or doping.

The AFe_2As_2 ($\text{A}=\text{Ba}, \text{Sr}, \text{Ca}$ or Eu) ("122") systems are prototype iron pnictide materials, since clean, large and homogeneous single crystals are available and various ways of tuning towards SC have been reported.²⁻⁴ EuFe_2As_2 is unique among them because it carries a local magnetic moment due to the divalent Eu atoms. It exhibits a combined transition of structural and SDW order of Fe magnetic moments at $T_0 = 190$ K and subsequently Eu 4f moments order below $T_N = 19$ K into a canted antiferromagnetic (AF) state.⁵⁻⁸ This state is characterized by a ferromagnetic (FM) alignment of the moments along the orthorhombic a -axis with AF coupling along c .⁶ Interestingly, the magnetic susceptibility above T_N , which is dominated by the fluctuating Eu^{2+} moments, displays a Curie-Weiss law, $\chi = \chi_0 + C/(T - \theta)$, with positive Weiss temperature, $\theta \sim 20$ K, despite the AF ground state.^{5,9} Indeed, the AF ground state could easily be switched to a FM state in small in-plane fields of order 1 T.⁹ These observations suggest that the Eu-system is close to a FM instability. Either the application of hydrostatic pressure to EuFe_2As_2 or the P-substitution on the As site in $\text{EuFe}_2(\text{As}_{1-x}\text{P}_x)_2$, which induces chemical pressure, suppress the T_0 transition and induce superconductivity.¹⁰⁻¹⁵ The superconducting (SC) transition reaches up to 30 K at the optimum pressure and P-substitution around 2.8 GPa and $x \approx 0.2$, respectively.¹¹⁻¹⁵ The magnetic ordering of Eu moments also changes its character as P is substituted. At low x a canting of the moments along the c -axis develops, which grows with increasing x , giving rise to a FM hysteresis in magnetization along the c -axis, while the system still dis-

plays an AF ground state.¹⁶ At $x > 0.23$ the Eu ordering switches to FM.¹¹

One of the important and controversially discussed issues in $\text{EuFe}_2(\text{As}_{1-x}\text{P}_x)_2$ is the interplay between superconductivity and Eu-FM ordering. In the past, Z. Ren *et al.* reported a SC transition at 26 K, followed by FM ordering of Eu magnetic moments at 20 K on polycrystalline samples of $\text{EuFe}_2(\text{As}_{0.7}\text{P}_{0.3})_2$ and discussed a bulk coexistence of both phenomena, which would have important consequences on the SC order parameter.¹⁰ Subsequent magnetic Compton scattering experiments on similar polycrystalline material indicated competition between the two phenomena.¹⁷ We have previously reported the phase diagram for single crystalline $\text{EuFe}_2(\text{As}_{1-x}\text{P}_x)_2$.¹¹ In contrast to the report on polycrystals, we found that single crystals with $x \geq 0.26$ are lacking bulk superconductivity. In this study we have carefully investigated the homogeneity of the P content by energy dispersive x-ray (EDX) microprobe analysis, since already a small inhomogeneity in the P content could lead to a seeming coexistence of SC and FM order, due to contributions from different volume fractions. Thus, any small inhomogeneity or deviation between the nominal and actual composition may explain the discrepancy to the experiments on polycrystals. However, three more recent studies on polycrystals also claim a much wider SC region for $0.2 \leq x \leq 0.4$ and concluded a bulk coexistence of superconductivity and FM order.¹⁸⁻²⁰ Since this issue may sensitively depend on inhomogeneities and sample quality which could vary with different P-substitutions, we decided to perform detailed hydrostatic pressure experiments on two selected well characterized P-substituted single crystals.

As shown below, we can perfectly map the hydrostatic pressure results to our previously determined phase diagram for single crystalline $\text{EuFe}_2(\text{As}_{1-x}\text{P}_x)_2$. In particular, we verify the peculiar extremely narrow existence range of bulk superconductivity and its suppression at the concentration $x = 0.23$ for which Eu magnetic order switches to FM. Additionally, we can relate this transition to a change of the electronic structure due to a Lifshitz transition, that meanwhile has been established by angular-resolved photoemission spectroscopy

(ARPES),²² as well as thermopower measurements.²³

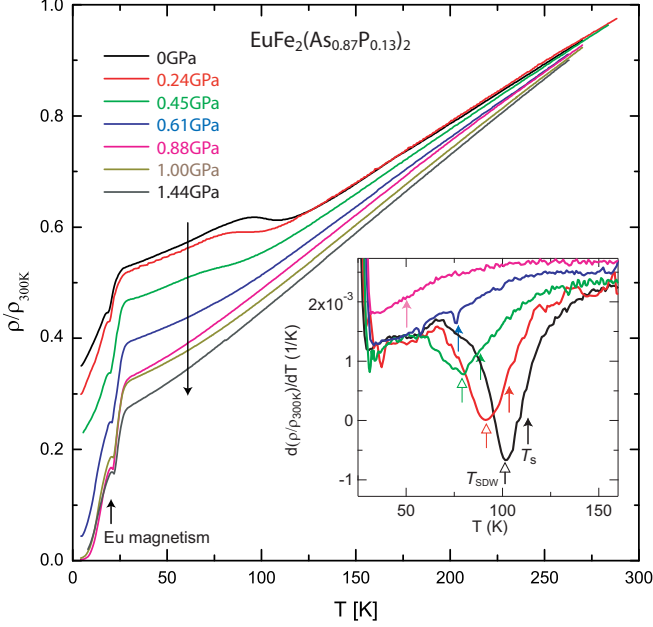


FIG. 1: (Color online) Electrical resistivity normalized by its value at 300 K, ρ/ρ_{300K} , for $\text{EuFe}_2(\text{As}_{0.87}\text{P}_{0.13})_2$ under hydrostatic pressure. The inset displays the temperature derivative of the resistivity $d\rho/dT$ vs. T . Arrows indicate T_s and T_{SDW} which are determined from the inflection points and minima, respectively.

Single crystals of $\text{EuFe}_2(\text{As}_{1-x}\text{P}_x)_2$ were grown by the FeAs self-flux method.¹¹ The homogeneity and actual composition of the two samples with $x = 0.13$ and $x = 0.18$ was confirmed within $\Delta x = 0.01$ error by EDX microprobe analysis on several points of cleaved surfaces. Powder X-ray analysis displays a compression of the unit cell volume, related to the chemical pressure effect of P substitution.¹¹ The temperature dependence of the electrical resistivity under hydrostatic pressure was measured by a standard four probe method with the current flowing in the tetragonal basal plane. The measurements were performed from room temperature down to 4.2 K and under hydrostatic pressure up to ~ 1.5 GPa by utilizing a CuBe piston-cylinder pressure cell. Daphne oil was used as pressure transmitting medium. The applied pressure was carefully determined by detecting the change of the SC phase transition temperature of a piece of Pb, placed in the pressure cell. From the observation of a pressure independent width of the Pb SC phase transitions, we conclude a good hydrostaticity of the pressure.

We first discuss measurements on a $x = 0.13$ single crystal displayed in Figure 1. The combined transition at $T_0 = 190$ K for the pure compound becomes separated into two transitions of structural (T_s) and SDW (T_{SDW}) order in P-substituted materials and their separation increases with increasing P-concentration.²¹ The temperature derivative of the electrical resistivity is a sensitive probe of the two phase transitions in 122 iron pnictides.

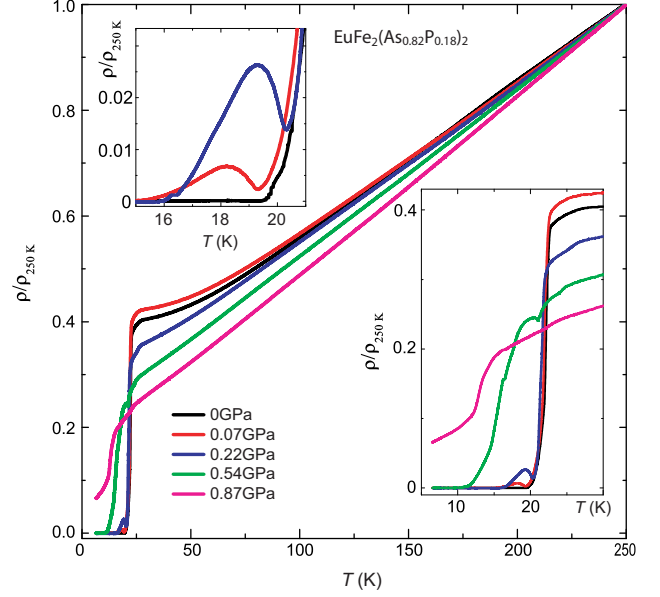


FIG. 2: (Color online) Electrical resistivity normalized by its value at 250 K, ρ/ρ_{250K} , for $\text{EuFe}_2(\text{As}_{0.82}\text{P}_{0.18})_2$ under hydrostatic pressure. The two insets enlarge the low temperature region.

As shown e.g. in Ref.²⁴, T_s and T_{SDW} are characterized by an inflection point and minimum in $d\rho/dT$ vs. T , respectively, compatible with thermodynamic, magnetic and structural experiments. The inset of Figure 1 displays the resistivity derivative of our data, together with arrows at the positions of the inflection points and minima. The signature of the SDW transition could only be resolved up to 0.45 GPa, while a very broadened anomaly related to the structural transition is detectable until 0.88 GPa. The positions of the so-derived transition temperatures in the phase diagram (Fig. 3) are discussed later. Around 30 K, a drop is found in $\rho(T)$, which however does not represent bulk superconductivity, since it is not accompanied by a Meißner signal in the magnetic susceptibility.¹¹ This signature is related to a very small SC volume fraction, likely due to some very small inhomogeneity, which could not be detected within the resolution of X-ray diffraction and EDX. With increasing pressure, the SC signal is getting more pronounced, reaching $\rho = 0$ at the highest pressure, indicating an increase of the SC volume fraction. At low temperatures, the resistivity also shows a hump, which is a signature of the Eu magnetic ordering.

We have performed similar hydrostatic pressure experiments on $\text{EuFe}_2(\text{As}_{0.82}\text{P}_{0.18})_2$, cf. Figure 2. This sample is a bulk superconductor at ambient pressure, confirmed by Meißner effect and specific heat measurements,¹¹ and displays a sharp and complete resistive SC transition at 22 K, i.e. slightly below the maximal T_c of 30 K found previously for a $x = 0.2$ single crystal.¹¹ Upon increasing the hydrostatic pressure, T_c does not increase, as one might have expected from the phase diagram of

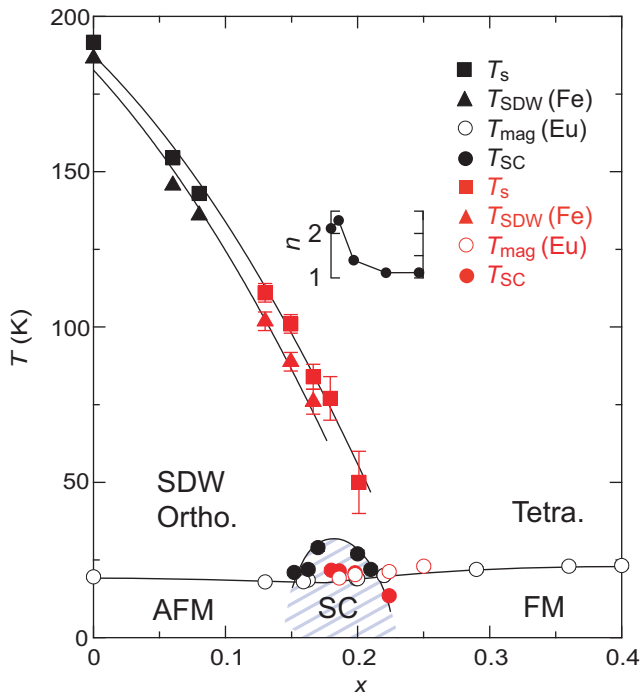


FIG. 3: (Color online) Phase diagram of $\text{EuFe}_2(\text{As}_{1-x}\text{P}_x)_2$, including data points from the previous ambient-pressure work (black symbols) and this study (red symbols). The effective P-concentration x for the data points from this study has been obtained by using the bulk modulus $B = 82.9 \pm 1.4$ GPa,²⁵ and the lattice constants of $\text{EuFe}_2(\text{As}_{1-x}\text{P}_x)_2$.¹¹ Lines are guides to the eye. The inset shows the exponent n of the temperature dependence of the electrical resistivity $\rho = \rho_0 + AT^n$ as a function of the calculated effective P-concentration for $\text{EuFe}_2(\text{As}_{0.82}\text{P}_{0.18})_2$ under hydrostatic pressure. It shares the horizontal axis for x of the main panel. The exponent n is obtained by fitting the data between 25 and 100 K.

$\text{EuFe}_2(\text{As}_{1-x}\text{P}_x)_2$.¹¹ Rather the SC transition becomes incomplete (cf. the inset), shifts towards lower temperatures and is suppressed at a pressure of 0.87 GPa. The incomplete SC transition also displays a signature at the ordering of Eu^{2+} local moments. In previous hydrostatic pressure experiments on EuFe_2As_2 , similar behavior has been found at pressures slightly below or above the pressure range of bulk superconductivity.^{12–14} The data thus indicate, that single crystalline $\text{EuFe}_2(\text{As}_{0.82}\text{P}_{0.18})_2$ is located just at the border of bulk superconductivity, which disappears at very low pressure.

In order to obtain a quantitative comparison between the pressure and P-substitution, we use the bulk modulus $B = 82.9 \pm 1.4$ GPa of BaFe_2As_2 , determined in the orthorhombic state at 33 K (Ref.²⁵) and the change of the lattice constants in $\text{EuFe}_2(\text{As}_{1-x}\text{P}_x)_2$.¹¹ Using these data, 0.61 GPa corresponds to 5% of P-substitution. Consequently, $\text{EuFe}_2(\text{As}_{0.87}\text{P}_{0.13})_2$ at a pressure of 0.61 GPa corresponds to $x = 0.18$ at ambient pressure. Indeed both data sets display similar cur-

vature above the SC transition (cf. Figs. 1 and 2), and increasing hydrostatic pressure for both concentrations leads to a more linear temperature dependence of $\rho(T)$. We fitted the resistivity data between 25 and 100 K to a simple power law form $\rho(T) = \rho_0 + AT^n$ and followed the evolution of the resistivity exponent n with pressure for the $x = 0.18$ single crystal, as shown in the inset of Fig. 3 (note, that the x-axis has been converted to the P content using the above relation). A quasi linear temperature dependence ($n \approx 1$), highlighting non-Fermi liquid behavior, is found for $x = 0.18$ at 0.54 and 0.87 GPa, which corresponds to $x = 0.224$ and $x = 0.25$ at ambient pressure, respectively. This is compatible with existing ambient-pressure data on $\text{EuFe}_2(\text{As}_{1-x}\text{P}_x)_2$ single crystals,^{11,21,23} which found $n \approx 1.2$ for $x = 0.2$, $n \approx 1$ for $x = 0.23$, and $n \approx 1.4$ for $x = 0.26$. The minimum of n near $x = 0.23$ is related to a change of the electronic structure at the concentration, discussed below. In addition, beyond this concentration, the previous ambient-pressure results have proven the suppression of bulk superconductivity (Ref.¹¹), which nicely agrees with the similar behavior for $x = 0.18$ under hydrostatic pressure above 0.54 GPa. This indicates an excellent agreement between previous ambient-pressure data on $\text{EuFe}_2(\text{As}_{1-x}\text{P}_x)_2$ and the new hydrostatic pressure experiments on the two selected P substitutions. It also confirms, that the narrow existence range of superconductivity in this system is not related to disorder introduced by the P-substitution. Rather it must be related to the change of the electronic and crystal structure with chemical pressure.

For the phase diagram, displayed in Figure 3, we have plotted the previous ambient-pressure phase transition temperatures together with that of our new hydrostatic pressure studies, where the pressure has been converted to an effective P concentration using the above relation. We have determined the SC T_c and the magnetic ordering temperature of the Eu^{2+} moments from the maxima in the temperature dependences of $d\rho/dT$ and ρ , respectively. Clearly, superconductivity is suppressed beyond $x = 0.23$, in perfect agreement with the previous study.¹¹ The phase transition temperatures T_{SDW} and T_s , determined for $x = 0.13$ under hydrostatic pressure, are also included to the phase diagram. The extrapolation of both transition temperatures towards absolute zero suggests that their complete suppression happens at $x > 0.2$, i.e. beyond the concentration for which T_c is maximal. This is corroborated by the evolution of the resistivity exponent $n(x)$, which has its minimum around $x = 0.23$. Thus, the optimum concentration for superconductivity $x = 0.2$ is still *within* the orthorhombic phase. For $\text{BaFe}_2(\text{As}_{1-x}\text{P}_x)_2$ a much wider SC region in the phase diagram has been found, also under pressure.^{26,27} Typically for 122 pnictide superconductors, the SC state is found on both sides of the extrapolated QCP where the SDW ordering and structural distortion vanish.³ In $\text{EuFe}_2(\text{As}_{1-x}\text{P}_x)_2$, by contrast, superconductivity becomes suppressed at the same concentra-

tion $x = 0.23$, where resistivity and TEP indicate the most drastic non-Fermi liquid behaviors.^{21,23}

The disappearance of iron SDW order is likely caused by a change of the Fermi surface nesting properties detected by ARPES.²² A non-rigid band shift evolution of the Fermi surface with chemical pressure has been found. Importantly, the inner hole-like Fermi surface near the Γ point shrinks to zero at $x \approx 0.23$.²² Indeed, TEP has found indication for a Lifshitz transition near this concentration, from a non-monotonic evolution of $S(x)$ at constant temperature.²³ Such a change of the electronic configuration may also influence the Eu^{2+} magnetic ordering, since density-functional-theory-based calculations have found almost similar ground state energies for the AF and FM configurations using the room-temperature lattice constants in this concentration range.¹¹ Since the Ruderman-Kittel-Kasuya-Yosida (RKKY) exchange coupling between the Eu^{2+} local moments is oscillatory with the distance, starting with a FM coupling at low distances, the general trend towards ferromagnetism under chemical pressure is expected. Interestingly, by using a minimal multiband model, it has recently been shown that the Fermi surface nesting has strong influence on the RKKY interaction.²⁸ Within the SDW phase, the gapping of the Fermi surface induces an anisotropy in the RKKY interaction and modifies its strength and oscillatory behavior with respect to that in the paramagnetic regime. Thus, the suppression of T_{SDW} and T_s near $x = 0.23$ is expected to strongly influence the RKKY exchange coupling between the Eu moments and likely the coincidence with the change from AF to FM order is not accidental. Since superconductivity is sup-

pressed by ferromagnetism, this also explains the disappearance of superconductivity at the same concentration.

To conclude, we have compared the previously determined phase diagram for $\text{EuFe}_2(\text{As}_{1-x}\text{P}_x)_2$ with hydrostatic pressure experiments on two selected $x = 0.13$ and $x = 0.18$ single crystals. Using the reported value of the bulk modulus and the measured change of the lattice constants with x , we could quantitatively map the hydrostatic to the chemical pressure in this system. Our pressure experiments confirm the extremely narrow SC dome in this system, which is very different to the respective phase diagram for $\text{BaFe}_2(\text{As}_{1-x}\text{P}_x)_2$,^{26,27} where superconductivity extends over large phase space regions. Our results are in clear contrast to previous reports on the coexistence of superconductivity with FM Eu ordering.^{10,18,19} The evolution of the electrical resistivity exponent $n(x)$ displays a minimum at $x = 0.23$. At this concentration, ARPES and TEP have detected a Lifshitz transition.^{22,23} The change of the electronic structure together with the structural change most likely modify the Eu-RKKY interaction such that the Eu magnetism switches from AF to FM ordering. Since FM order is incompatible with superconductivity, this explains the peculiar phase diagram of $\text{EuFe}_2(\text{As}_{1-x}\text{P}_x)_2$, where a SC phase only exists in a very narrow regime.

Collaboration and valuable discussions with M. Dressel, J. Fink, C. Geibel, S. Jiang, D. Kasinathan, J. Maiwald, M. Nicklas, H. Rosner, S. Thirupathaiah, K. Winzer, D. Wu, and S. Zapf are gratefully acknowledged. This work has been supported by the DFG priority program SPP 1458.

-
- ¹ Y. Kamihara, T. Watanabe, M. Hirano and H. Hosono, *J. Am. Chem. Soc.* **130**, 3296 (2008).
 - ² D.C. Johnston, *Adv. Phys.* **59**, 803 (2010).
 - ³ J. Paglione and R.L. Greene, *Nature Phys.* **6**, 645 (2010).
 - ⁴ G.R. Stewart, *Rev. Mod. Phys.* **83**, 1589 (2011).
 - ⁵ Z. Ren et al., *Phys. Rev. B* **78**, 052501 (2008).
 - ⁶ Y. Xiao et al., *Phys. Rev. B* **80**, 174424 (2009).
 - ⁷ H.S. Jeevan, Z. Hossain, Deepa Kasinathan, H. Rosner, C. Geibel, and P. Gegenwart, *Phys. Rev. B* **78**, 052502 (2008).
 - ⁸ H.S. Jeevan, Z. Hossain, Deepa Kasinathan, H. Rosner, C. Geibel, and P. Gegenwart, *Phys. Rev. B* **78**, 092406 (2008).
 - ⁹ S. Jiang et al., *New J. Phys.* **11**, 025007 (2009).
 - ¹⁰ Z. Ren et al., *Phys. Rev. Lett.* **102**, 137002 (2009).
 - ¹¹ H.S. Jeevan, D. Kasinathan, H. Rosner, and P. Gegenwart, *Phys. Rev. B* **83**, 054511 (2011).
 - ¹² C.F. Miclea et al., *Phys. Rev. B* **79**, 212509 (2009).
 - ¹³ N. Kurita et al., *Phys. Rev. B* **83**, 214513 (2011).
 - ¹⁴ K. Matsubayashi et al., *Phys. Rev. B* **84**, 024502 (2011).
 - ¹⁵ T. Terashima et al., *J. Phys. Soc. Jpn.* **78**, 083701 (2009).
 - ¹⁶ S. Zapf, D. Wu, L. Bogani, H.S. Jeevan, P. Gegenwart, and M. Dressel, *Phys. Rev. B* **84**, 140503(R) (2011).
 - ¹⁷ A. Ahmed et al., *Phys. Rev. Lett.* **105**, 207003 (2010).
 - ¹⁸ I. Nowik, I. Felner, Z. Ren, G.H. Cao, and Z. A. Xu, *J. Phys.: Condens. Matter* **23**, 065701 (2011).
 - ¹⁹ G. Cao, S. Xu, Z. Ren, G.H. Cao, and Z.A. Xu, *J. Phys.: Condens. Matter* **23**, 464204 (2011).
 - ²⁰ J. Munevar et al., arXiv:1105.1201.
 - ²¹ S. Jiang, H.S. Jeevan, J. Dong, and P. Gegenwart, arXiv:1210.2634.
 - ²² S. Thirupathaiah et al., *Phys. Rev. B* **84**, 014531 (2011).
 - ²³ J. Maiwald, H.S. Jeevan and P. Gegenwart, *Phys. Rev. B* **85**, 024511 (2012).
 - ²⁴ I.R. Fisher, L. Degiorgi, and Z. Shen, *Rep. Prog. Phys.* **74**, 124506 (2011).
 - ²⁵ R. Mittal et al., *Phys. Rev. B* **83**, 054503 (2011).
 - ²⁶ S. Kasahara et al., *Phys. Rev. B* **81**, 184519 (2010).
 - ²⁷ L.E. Klintberg et al., *J. Phys. Soc. Jpn.* **79**, 123706 (2010).
 - ²⁸ A. Akbari, I. Eremin, and P. Thalmeier, *Phys. Rev. B* **84**, 134513 (2011).